Vol. 22, Nos. 5–6, September–November 2007 ISSN 0886-7798

Original research, innovations and case studies in the development of tunnelling, trenchless technology and underground space

Tunnelling and Underground Space Technology

incorporating **Trenchless Technology Research**

Editors: Einar Broch (Norway); Chris Rogers (UK); Raymond Sterling (USA); Jian Zhao (Switzerland)

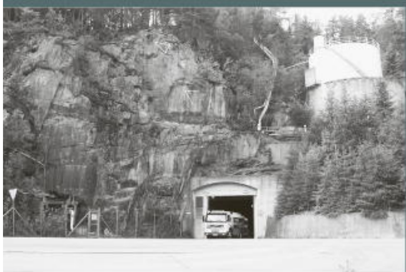

Special Issue
Trenchless Technology

Guest Editors
C. D. F. Rogers, R. L. Sterling and S. T. Ariaratnam

www.elsevier.com

Available online at ScienceDirect
www.sciencedirect.com

Available online at www.sciencedirect.com
ScienceDirect
Tunnelling and Underground Space Technology 22 (2007) 655–665
Tunnelling and Underground Space Technology incorporating Trenchless Technology Research
www.elsevier.com/locate/tust

Numerical modeling of tight fitting flexible liner in damaged sewer under earth loads

T.C. Michael Law [a], Ian D. Moore [b,*]

[a] *Mueser Rutledge Consulting Engineers, 14 Penn Plaza, 225 W. 34th Street, New York, NY 10122, United States*
[b] *Infrastructure Engineering, GeoEngineering Centre at Queen's – RMC, Queen's University, Kingston, Ont., Canada K7L 3N6*

Available online 27 February 2007

Abstract

Finite element analysis and closed form solutions are used to investigate and interpret tests conducted on a damaged rigid pipe fitted with an HDPE pipe liner. Details of the analysis are described, including the modeling of local interactions between the liner and the host pipe, different segments of the damaged host pipe across longitudinal fractures, and the host pipe and the surrounding ground. Laboratory tests on a lined sewer pipe under earth loads are studied to establish whether finite element and closed form solutions for the repaired pipe system are able to effectively represent the observed behaviour.

The deteriorated rigid pipe is fractured into four fragments, and these interact to impose pairs of closely spaced vertical line loads at the crown and invert of the liner. The finite element analysis demonstrates that significant local bending develops in the liner under these contact forces. Very little thrust develops in the liner, which is almost in pure bending provided the host pipe can still carry hoop thrust across fractures. The angular expansion of the fractures at crown and invert had a negligible effect on the local bending in the liner, allowing the use of theory for rings under parallel plate loading to provide simple calculations of liner response.

Nonlinear finite element analyses indicate that the interface between the liner and the host pipe is close to the full-slip (or smooth) condition. Analysis results for that condition are within 10% of the measured values. The finite element procedure also indicates that the host pipe and the liner within it deform under the effect of the full overburden pressure if the host pipe fractures after the liner is installed. Safe liner design could be achieved by ensuring that local bending associated with host pipe fracture and deformation under the full overburden pressures does not exceed tensile capacity of the polymer (in addition to liner design to resist buckling under external fluid pressure, in accordance with previous liner stability studies). Alternatively, measures might be used to avoid local bending in the liner by preventing deterioration of the host pipe and the surrounding soil during the design life of the repair.

Keywords: Polymer liners; Earth loads; Limit state; Local bending; Fractured sewers; Gravity pipe repair

1. Introduction

There is a growing need to develop reliable and cost effective rehabilitation techniques as our buried pipe infrastructure deteriorates. Pipe relining has emerged as one of the important repair methods for gravity flow storm-water and waste-water sewers. By inserting a flexible liner, the hydraulic integrity of a fractured sewer ('host') pipe can be restored.

It is well understood that buckling of the liner under the external fluid pressures is an important stability limit state as groundwater penetrates through fractures and open joints in the host pipe (e.g. Falter and Klein, 1989; El-Sawy and Moore, 1998). Flexible liner design standards like ASTM F1216 (1998) also consider buckling under earth loads as one of the performance limits, using buried pipe buckling theory that neglects the presence of the host pipe. Laboratory tests on lined damaged sewers reported by Law (2004) demonstrate that where earth pressures keep the segments of old sewer pipe in direct contact across fractures, significant hoop thrust cannot develop in the liner as a result of earth loads. In this case, the liner cannot buckle

* Corresponding author. Tel.: +1 613 533 3160; fax: +1 613 533 2128.
E-mail addresses: mlaw@mrce.com (T.C.M. Law), moore@civil.queensu.ca (I.D. Moore).

0886-7798/$ - see front matter © 2006 Elsevier Ltd. All rights reserved.
doi:10.1016/j.tust.2006.11.006

under earth loads. However, local bending develops in the liner due to the static response of the host pipe–liner system under earth load. Law and Moore (2003) indicate that significant circumferential tensile strains develop at both the crown and invert of the liner, as a result of local contacts between the host pipe segments and the liner. This local bending may cause cracking in the polymer liner if not considered in the design.

Following a discussion of the deformation mechanics of the repaired sewer system, recent numerical studies which examine the behaviour of liner systems are reviewed. Finite element procedures to model the deformation mechanics of the host-pipe liner system are then developed. Numerical results are compared to the laboratory data presented by Law (2004). The numerical analysis is then used to examine modeling of the interface between liner and host pipe, local geometry of the contact forces on the liner at the crown and invert, the effectiveness of closed form solutions for bending in the liner, and the liner response to overburden pressures if the rigid host pipe fractures and deforms after the liner is installed.

2. Mechanics of soil–host pipe–liner behaviour

2.1. Repaired sewer pipe components

There are three components involved in the static response of a repaired sewer pipe. They are the soil, the host pipe, and the liner (Fig. 1). The soil transfers load to the host pipe–liner system. It has been demonstrated by Law (2004) that deformation of a fractured sewer fitted with a flexible liner is controlled by the surrounding soil. Therefore, the soil also provides support to the repaired sewer pipe, to resist deformations.

The host pipe being repaired is typically rigid, and is usually made of vitrified clay or concrete. Host pipes with "overloading fractures" (Young and Trott, 1984) are the focus of attention in this study, Fig. 2. These fractures are longitudinal and are located along the crown, invert, and springlines of the host pipe (Falter, 2004). As demonstrated by Law (2004), the bending stiffness of the rigid host pipe is compromised after these overloading fractures occur. However, the host pipe will retain its hoop stiffness as long as the individual segments of fractured pipe remain in direct contact with each other.

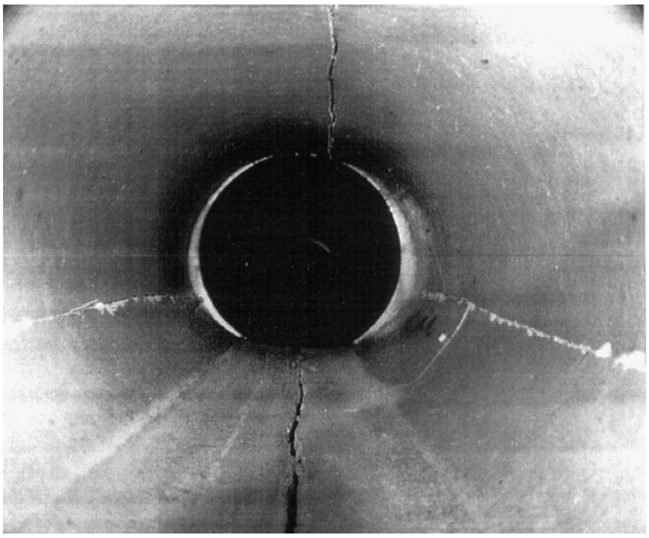

Fig. 2. Rigid pipe with overloading fractures (ATV-M 143-2, with permission).

The fracture pattern separating the pipe into four identical 90° segments represents the most flexible configuration that can form, that is the one with the least resistance to nonuniform earth loading. Since this represents the worst-case scenario that leads to the greatest fractured pipe deformations, this fracture configuration is considered in the present study. The liner installed is usually a plain or profiled flexible pipe composed of high density polyethylene (HDPE), polyvinylchloride (PVC), or resin impregnated fabric.

2.2. Kinematics and effect of local bending

A "tight fitting" host pipe–liner system is considered in this study (denoted close fitting in EN 13689, 2002). The host pipe being repaired is still capable of carrying hoop thrust, and the liner is installed within the host pipe after

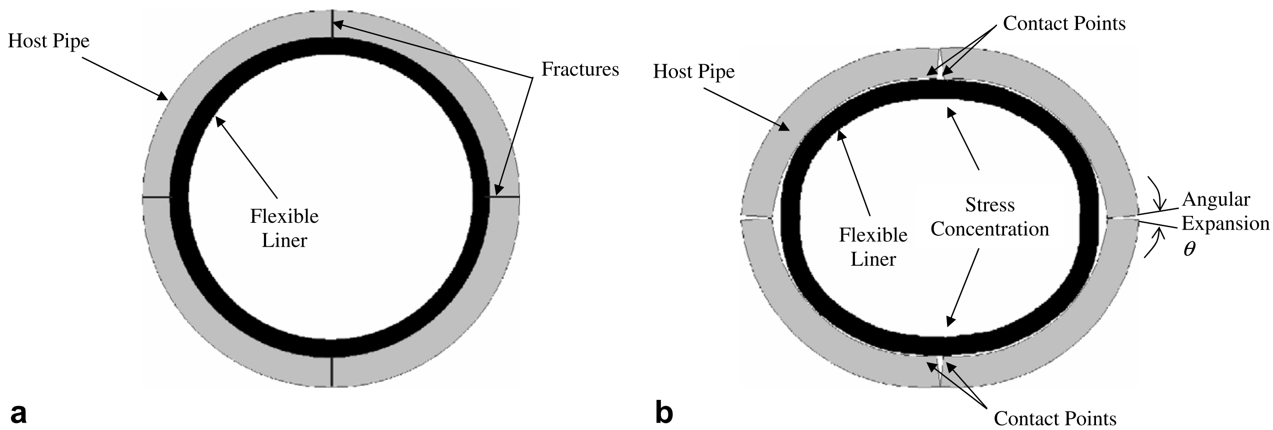

Fig. 1. Host pipe–liner system. (a) Undeformed and (b) Deformed.

construction without a gap between them. This configuration can develop when the damaged sewer is repaired by typical construction techniques such as slip-lining (when the initial gap is grouted), cured-in-place, and deform-reform (also known as fold–unfold or fold and form) techniques.

When a tight fitting host pipe–liner system is subjected to ground disturbance, the fractures in the host pipe expand at the inner surfaces of the host pipe at the crown and invert, and the outer surfaces at the springlines (Fig. 1b). However, contact at one point on the host pipe wall is maintained at each fracture, forming a hinge mechanism. The host pipe is still capable of carrying hoop thrust through those contacts despite deformations, Law (2004). The "separating" motion at the fractures in the host pipe puts the inner edges of the host pipe in direct contact with the external surface of the liner at both crown and invert. These contacts at the crown and invert result in two pairs of concentrated loads being imposed on the liner. Laboratory tests reported by Law and Moore (2003) show that these local contacts cause a substantial increase in tensile circumferential strains on the inner surface of the liner. When the liner is encased in a host pipe that can still carry thrust, the liner responds in almost pure bending as the repaired pipe deforms under earth loads. Without significant hoop thrust, buckling of the liner is not possible.

An angle, θ, is used here to quantify the "angular expansion" of the fractures. The flexural response of this host pipe–liner system, where the fractures are longitudinal to the pipe axis, is governed by plane strain conditions, Law (2004).

3. Laboratory measurements of local strains caused by host pipe–liner deformations

The objective is to develop a numerical model that captures the deformation shape of the host pipe-line system and local bending in the liner. This model is then used to study the behaviour of repaired sewer pipes. It is valuable to review the literature to locate data suitable for comparison with the numerical results, to permit evaluation of the quality of the computer modeling.

The soil–host pipe–liner interaction was studied by Doll (2001) using full-scale laboratory testing. The tests featured burial of a repaired pipe sample within a compression test cell. Local strain measurements in the liner were obtained using strain gauges placed on the inner surface of the liner at the crown and springlines. Since matching strain gauges were not applied at the outer surface of the liner, it is not possible to calculate hoop strain and thrust, or curvature change and moment. That makes it difficult to assess the quality of the test results, and difficult to use that data for computer model evaluation.

Takahashi et al. (2002) studied bedding effects on the tight fitting flexible liner with both full-scale laboratory testing and centrifuge model testing. The full-scale laboratory tests involved an HDPE liner encased within a host pipe, which was reassembled from many broken pieces of a rigid earthenware pipe. The sample was buried in sand in a 1.0 m by 1.0 m by 1.0 m test cell, and pressure was applied from the top of the backfill using a hydraulic jack. For the centrifuge tests, the host pipe was made out of aluminum alloy and a PVC pipe was used as the liner. From the test data, it is not clear whether bending strain is enhanced or decreased due to the presence of the host pipe, since the number of strain gauges was inadequate to record local strain concentrations.

Table 1
Soil parameters for the test

Applied pressure (kPa)	Modulus[a] (kPa)	K_0	$\upsilon_s = \frac{K_0}{1+K_0}$
30	1550	0.47	0.32
60	1910	0.48	0.32
90	2300	0.48	0.33
105	2490	0.49	0.33
120	2660	0.49	0.33
135	2800	0.50	0.33
150	2950	0.50	0.33
165	3190	0.50	0.33

[a] Secant Young's Modulus.

Law (2004) undertook laboratory tests featuring a host pipe, with outer diameter of 370 mm and thickness of 25 mm, cast from concrete and pre-fractured at the crown, invert, and springlines. A plain HDPE with diameter of 320 mm, and diameter to thickness ratio (SDR) of 26, was used as the liner. It was instrumented with displacement transducers and resistance strain gauges at two test sections to measure diameter changes and local strains. Displacement transducers were also installed in the host pipe to monitor horizontal diameter change and relative movement of the host pipe segments, so that angular expansion can be calculated.

A test on the repaired pipe sample was performed in a biaxial compression test cell (Brachman et al., 2001). Soil parameters were measured independently during the test and the results are summarized in Table 1.

Law's study demonstrated that the circumferential strains in the liner were increased by approximately 50% at the crown and invert due to the local contacts between the host pipe and the liner, Fig. 1b. Strain readings of the liner at the inner and the outer surfaces across host pipe fractures were almost equal and opposite. These indicate that the liner was responding in almost pure bending at those locations when the host pipe was present.

Since the laboratory tests reported by Law (2004) represent the only available data where both deformations and local bending are monitored in the liner, the numerical analysis reported here was developed using comparisons with those laboratory tests.

4. Review of numerical analysis of lined sewer pipe

Takahashi et al. (2002) modeled their laboratory tests, mentioned in the previous section, using linear elastic finite element analysis. Soil moduli and Poisson's ratios were not measured in the tests; instead they were back calculated using changes in vertical liner diameter. The pipe–soil interface was modeled using joint elements with low tangential stiffness (an empirical choice of 1 kPa). The fractures in the host pipes were not modeled explicitly; rather the deteriorated condition was captured by altering its Young's modulus. They report that the computer results showed good agreement with the laboratory results.

The finite element analysis carried out by Takahashi et al. (2002) provided vertical pipe diameter changes that matched the mean laboratory result, since soil modulus was calibrated to ensure this was so. However, this analysis cannot be expected to provide reasonable estimates of horizontal diameter change or effective calculations of local bending in the liner, since the "smeared damage modulus" approach cannot effectively capture the development and influence of local contacts between the host pipe and the liner.

Du (1999) used finite difference analysis to study the effect of liner materials on soil–host pipe–liner interaction. His study followed the current design standards, and focused on the buckling capacity of the liner, and ignored the presence of the host pipe. Since the host pipe was not represented, that analysis cannot capture the kinematics of the host pipe–liner response such as local liner bending.

Explicit representation of the fractured host pipe and the liner within it is needed to:

(a) Effectively model the interaction between the separate segments of the host pipe.
(b) Capture the interaction between the host pipe segments and the liner.
(c) Capture the response of the host pipe in the soil.

5. Finite element analysis of repaired pipe alone

5.1. Host pipe–liner interaction analysis

Falter (2004) describes finite element calculations used in the design of pipe liners to ATV M-127-2 (2000) where one quadrant of a fractured host pipe and the liner within it are modeled and local bending stresses are evaluated in the liner. These calculations for the liner and host pipe are conducted representing the surrounding ground using independent elastic (i.e. Winkler) springs. His analysis illustrates the value of considering the structural response (or kinematics) of liner-host pipe deformations.

The deformation mechanisms of the host pipe–liner system are therefore studied using the finite element program AFENA (Carter and Balaam, 1980). Modeling techniques for the host pipe segments are discussed by Law (2004). Similar procedures have been adopted here. Since the focus of this study is to capture the kinematics of the host pipe–liner system and calculate the circumferential stress through the thickness of the liner, six-node triangular elements have been employed. If the local contact stresses in the host pipe fragments or the radial contact pressures between the host pipe and the liner were the subject of

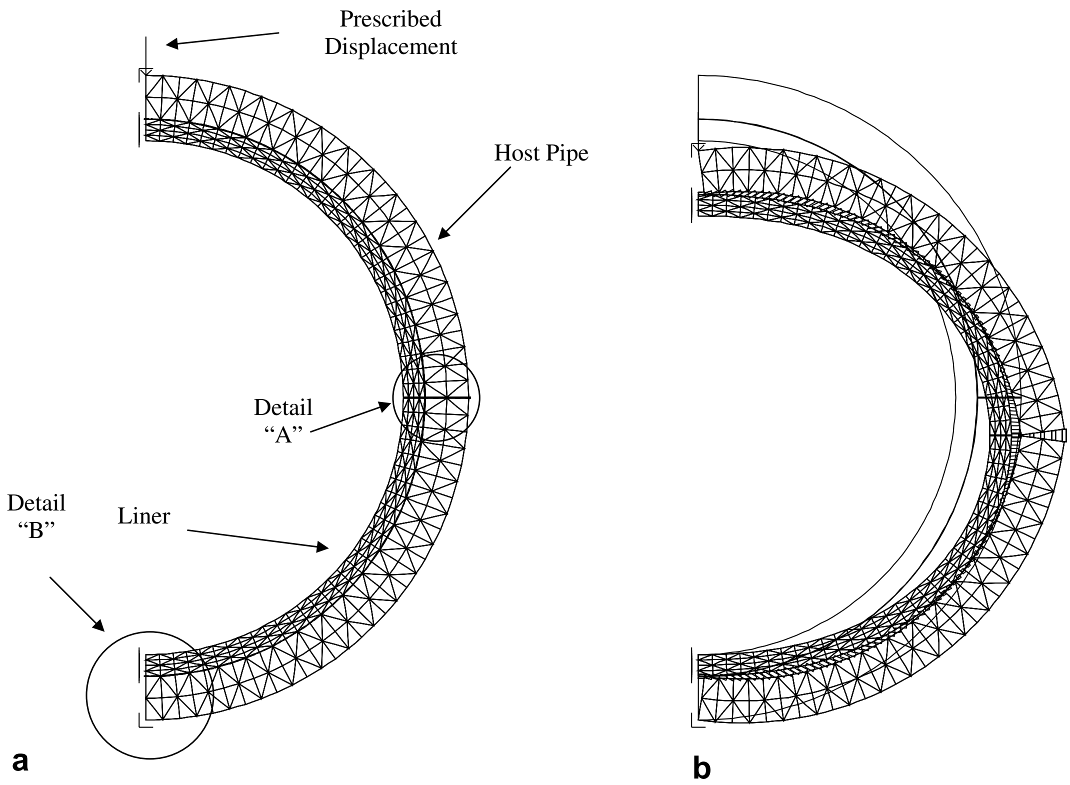

Fig. 3. Host pipe–liner finite element mesh. (a) Undeformed and (b) Deformed (Exaggerated).

interest, then a more refined mesh or higher order elements would likely be required.

Only half of the repaired pipe system has been analyzed due to the symmetry of the problem, Fig. 3. Two-dimensional plane strain analysis was employed since the flexural response of the prismatic host pipe–liner system is planar. Two hundred and forty six-node triangular elements were used to model half of the host pipe (two 90° segments). The host pipe was modeled as 24.75 mm thick, 0.25 mm less than the test specimen to accommodate joint elements between the host pipe and the liner (this geometry change does not have a significant effect on the calculated response). The outer diameter of the host pipe was modeled as 370 mm, identical to the test sample.

To model the kinematics of the fracture at the crown and invert of the host pipe, the outer edge of the fracture was fixed in the horizontal direction, since the "hinge" is located at the exterior surface, Fig. 3b. As a result, that node can only move vertically, while allowing the fracture to open at the inner surface. The outer surface of the host pipe at the invert was also provided with a vertical fixity, to fix the system and ensure vertical equilibrium, Fig. 3a.

To model the fractures at the springlines, a 0.5 mm gap was left between the two 90° pipe segments, and joint elements were used to connect them, Fig. 4a. From Fig. 3, the "hinges" at the springline of the host pipe is at the inner edge; therefore, that particular joint element was specified with high normal stiffness and high shear stiffness. Therefore, the inner edges of the two host segments maintain contact across the springline fracture even when the pipe deforms. To allow the fracture to open without any resistance, the remaining joint elements were assigned negligible normal and shear stiffnesses. These joints with negligible stiffnesses have no effect on the calculation results, and could have been removed from the analysis.

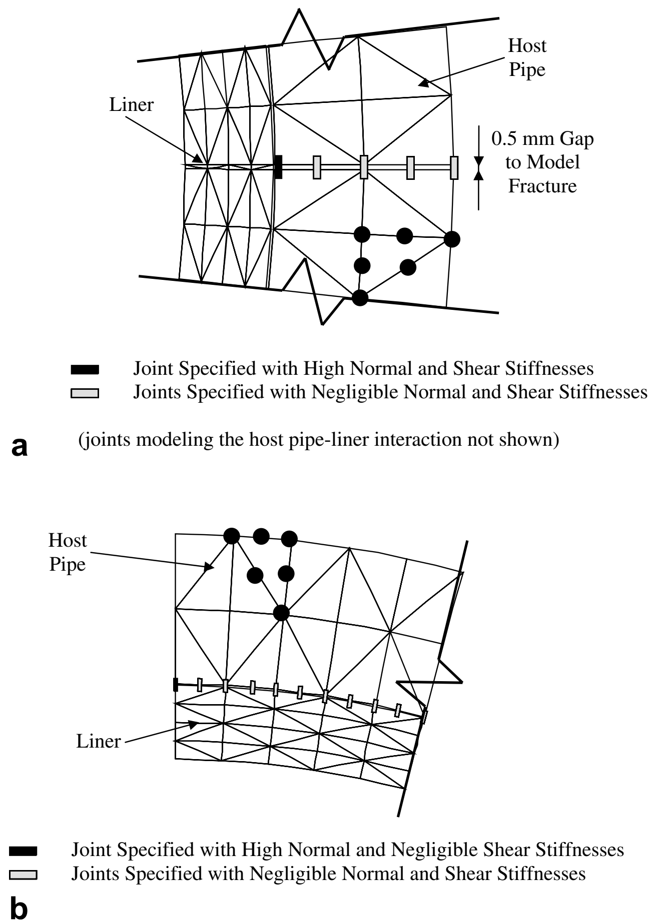

Fig. 4. Host pipe–liner interaction modeling at springline and invert (crown). (a) Detail "A" and (b) Detail "B".

Four hundred and eighty eight six-node triangular elements were used to model the flexible HDPE liner. The dimensions of the liner were specified so that they match the liner sample used in the laboratory tests (thickness = 12.3 mm and outer diameter = 320 mm). As discussed, a 0.25 mm gap was left between the host pipe and the liner to accommodate the joint elements that connect them. Two different types of joints were used to model the interaction between the host pipe and the liner. Joints with high normal stiffness and negligible shear stiffness were used at the crown and invert, where local contacts between the host pipe and liner are expected (Fig. 4b). As a result, the inner surfaces of the host pipe fractures can expand, yet stresses can be transferred to the liner. The rest of the joint elements were specified with negligible normal and shear stiffnesses, once it was established that these points do not remain in contact (that is, a gap forms across the elements).

The host pipe segments were specified with typical concrete or clay properties (Young's modulus, $E_{\text{host}} = 30$ GPa, Poisson's ratio, $\upsilon_{\text{host}} = 0.3$). The modulus of the host pipe has no effect on the calculated response, since it is essentially rigid compared to soil. For the HDPE liner, elastic modeling using secant modulus is the simplest and most widely used approach. Dhar and Moore (2000) demonstrated that the elastic model can successfully capture the behavior of a buried thermoplastic pipe when the strain level in the pipe remains low. The secant modulus for the HDPE liner was chosen as 600 MPa based on the duration of the experiment (2.5 h) using the HDPE models of Moore and Hu (1996). A typical Poisson ratio for HDPE ($\upsilon_{\text{liner}} = 0.46$) was also employed.

Vertical displacement was prescribed at the outer surface of the host pipe at the crown in 1.4 mm increments producing deformed shapes like that shown in Fig. 3b. Ten such increments were applied, resulting in a 14.4 mm decrease in vertical diameter (ΔD_{v}), identical to the maximum value observed in the test. At each increment, the changes in host pipe diameters ($\Delta D_{\text{v-host}}$ and $\Delta D_{\text{h-host}}$), the changes of the liner diameters ($\Delta D_{\text{v-liner}}$ and $\Delta D_{\text{h-liner}}$), and the corresponding angular expansions were recorded and compared. The finite element results are summarized in Tables 2 and 3.

Table 2 shows that despite the fractures that open up at the inner surface of the host pipe at the crown and invert, the decrease in vertical diameters of the host pipe and the liner are essentially identical, $\Delta D_{\text{v-host}} = \Delta D_{\text{v-liner}}$ (as fracture

Table 2
Finite element analysis results, deformation of the repaired pipe system

Increment no.	Prescribed Displacement (mm)	Host pipe[a]		Liner[a]	
		$\Delta D_{\text{v-host}}$ (mm)	$\Delta D_{\text{h-host}}$ (mm)	$\Delta D_{\text{v-liner}}$ (mm)	$\Delta D_{\text{v-liner}}$ (mm)
0	0	0	0	0	0
1	1.44	−1.44	1.60	−1.44	1.31
2	2.88	−2.88	3.21	−2.88	2.62
3	4.32	−4.32	4.81	−4.32	3.94
4	5.76	−5.76	6.42	−5.76	5.25
5	7.20	−7.20	8.02	−7.20	6.56
6	8.64	−8.64	9.62	−8.64	7.87
7	10.1	−10.1	11.2	−10.1	9.18
8	11.5	−11.5	12.8	−11.5	10.5
9	13.0	−13.0	14.4	−13.0	11.8
10	14.4	−14.4	16.0	−14.4	13.1

[a] Negative indicates decrease.

Table 3
Finite element analysis results, kinematics of the host pipe

Increment no.	Prescribed displacement (mm)	$\theta_{\text{cr}} = \theta_{\text{inv}}$	θ_{sp}
0	0	0	0
1	1.44	0.5°	0.5°
2	2.88	1.0°	1.0°
3	4.32	1.5°	1.5°
4	5.76	2.0°	2.0°
5	7.20	2.5°	2.5°
6	8.64	3.0°	3.0°
7	10.1	3.5°	3.5°
8	11.5	4.0°	4.0°
9	13.0	4.5°	4.5°
10	14.4	5.0°	5.0°

angular expansion increases, a slight difference develops). On the other hand, the increase in horizontal diameter is higher for the host pipe than the liner (16.0 mm compare to 13.1 mm) creating a gap between them at the springlines. This gap was also observed in the laboratory test.

In the host pipe–liner test, at the highest test pressure of 165 kPa, a vertical pipe deformation of 14.4 mm was measured, and the corresponding horizontal deformations were 16.0 mm for the host pipe and 12.5 mm for the liner. The finite element analysis results therefore match the laboratory measurements reasonably well.

Law (2004) describes the geometrical relationship between the vertical and horizontal diameter changes of a rigid pipe broken into four segments as a result of overloading fractures. The use of that model can be extended to describe the kinematics of the host pipe with a liner encased within. The presence of the liner has no effect on the host pipe kinematics. Law (2004) presents a closed form analysis of the kinematics of a rigid pipe featuring planar, longitudinal fractures at its crown, invert and springlines. Equations numbered 2.1–2.6 by Law (2004) quantify the changes in vertical and horizontal diameters as a function of the angles of fracture opening at crown and invert (assuming the segments remain in contact at the external pipe surface), and at the springlines, where it is assumed that contact occurs at the inner surface. Those equations were used to evaluate the host pipe deformations calculated by the finite element analysis, which provided identical results.

Table 3 shows that angular expansion at the fractures at crown, invert, and springlines are identical at each increment, and θ remains low even at the highest vertical pipe deformations. The measured fracture angular expansion in the test was 5° at 14.4 mm of vertical pipe deformation. The laboratory and the finite element analysis results match well.

As shown in Figs. 1b and 3b, local contacts between the host pipe and the liner are expected at the crown and invert. Examination of the typical deformed shape illustrated in Fig. 3b reveals that for the liner configuration and deformation levels studied here, there is no other contact between the host pipe and the liner besides those at the crown and invert, though contact almost occurs at the 2 o'clock and 4 o'clock positions. In addition, the small angular expansion implies that the two pairs of forces acting on the liner can be approximated by one force at the crown and one force at the invert, similar to a ring under parallel plate loading. This allows the use of a simplified theoretical solution to calculate the response of the liner when it is encased in the host pipe, as discussed in a subsequent section.

Small-strain deformations were assumed in the finite element analysis reported here. However, geometrically nonlinear analysis (large strain analysis) was also carried out and the results were virtually identical.

5.2. Finite element analysis of local bending in the liner

Circumferential stresses were calculated in the liner at the crown, invert, and springlines using the finite element analysis. The distribution of circumferential stresses across the liner thickness at the crown at the highest ΔD_v of 14.4 mm is shown in Fig. 5 (tension positive). It reveals that the circumferential stress is linear across the thickness of the liner, where the inner surface is in tension and outer surface is in compression. Fig. 5 also shows that circumferential stress at the neutral axis is zero, indicating that the liner is responding in pure bending, and hoop thrust is negligible. Stress distributions were also studied at the springline. At this location, a small hoop thrust also develops, equal to half the vertical force applied at the crown. This thrust is small in comparison with the bending moment, and stress and strain distributions like those illustrated in Fig. 5 revealed that the hoop stresses resulting from the thrust in the liner were small compared to the bending stresses.

The circumferential stress values at the integration points were interpolated to the section of interest, then extrapolated to the liner extreme fibers. The results from each prescribed displacement increment are plotted against the pipe deformations on Fig. 6a and b. Extreme fiber stresses at the crown and invert are plotted against

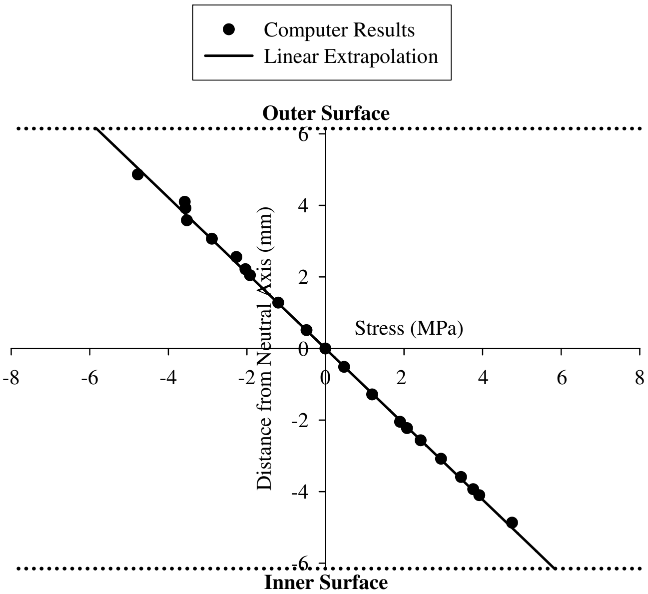

Fig. 5. Circumferential stress at crown of the liner (tension +ve).

$\Delta D_{\text{v-liner}}$, and results at the springlines are plotted against $\Delta D_{\text{h-liner}}$. The results show that the magnitude of circumferential stress in the liner increases linearly with liner diameter change.

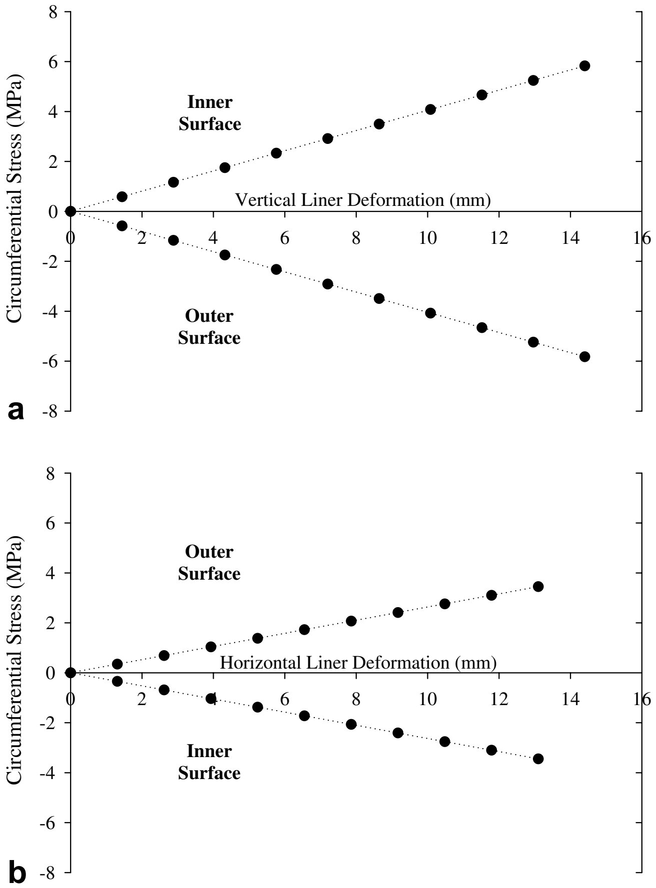

Fig. 6. Extreme fiber stresses in the liner as a function of diameter decrease (tension +ve). (a) Crown and invert and (b) Springlines.

Extreme fiber stresses are substantially higher at the crown and invert. At the highest vertical pipe deformation ($\Delta D_v = 14.4$ mm), bending stresses at the crown and invert are ±5.8 MPa, compared to ±3.4 MPa at the springlines.

Using the liner modulus of 600 MPa and Poisson's ratio of 0.46, circumferential strains in the liner can be calculated, and the results are shown on Fig. 7a and b. Laboratory measurements of strain are also shown in the figures. Measured strains shown here have been adjusted up by the factor of 1.43 developed by Brachman (1999) to account for wall stiffening caused by the adhesive used when gluing strain gauges onto HDPE. A comparison with the strain measurements at the crown and invert indicates that the finite element results matched the measured bending strains within 9% (Fig. 7a). One likely reason for the discrepancy is the limitation of the finite element analysis in calculating stresses at the centreline of the pipe. At the springlines, the finite element analysis yields better agreement, since the discrepancy between the calculated and measured values is about 0.5% (Fig. 7b).

As discussed in the previous section, the response of the liner encased in a host pipe is similar to a ring under parallel

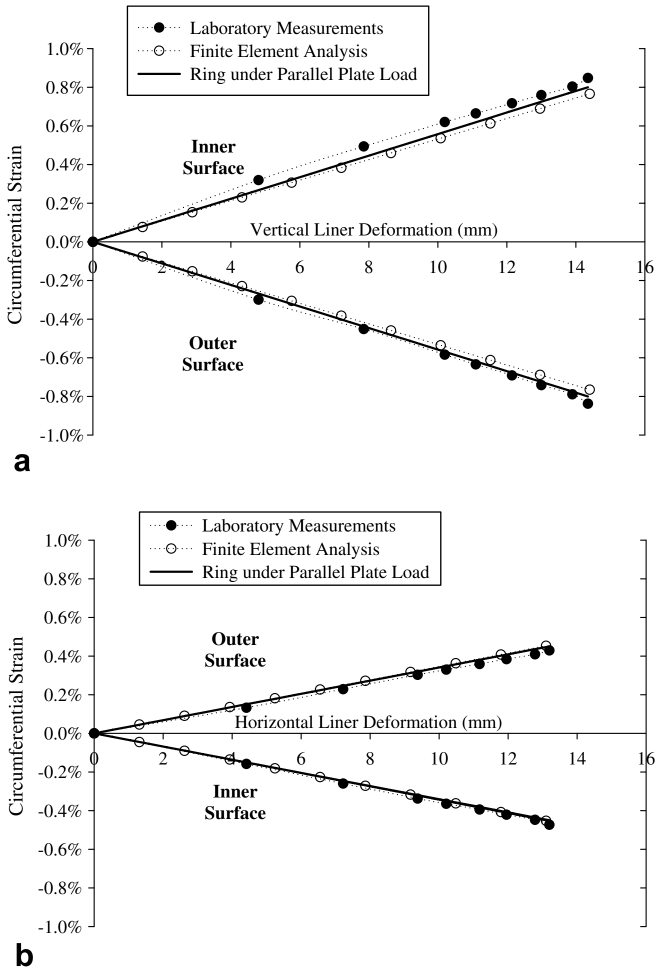

Fig. 7. Circumferential strain in liner at the extreme fibers as a function of diameter decrease; tension +ve; measurements, finite element and ring theory results. (a) Crown and invert (+ve tension) and (b) Springlines.

plate load for the level of deformation studied. Law and Moore (2003) developed an equation for bending strains in the liner at crown and invert, using ring theory. Results from that approximation are included in Fig. 7a and b. This makes it clear that the parallel plate load approximation of Law and Moore (2003) is very effective for this particular lined sewer problem.

Though this finite element analysis does not involve the backfill soil, the kinematic response of the repaired pipe obtained from this analysis would be identical to the buried pipe response. The calculated bending strains in the liner are independent of the liner modulus, since prescribed displacement was used in the analysis.

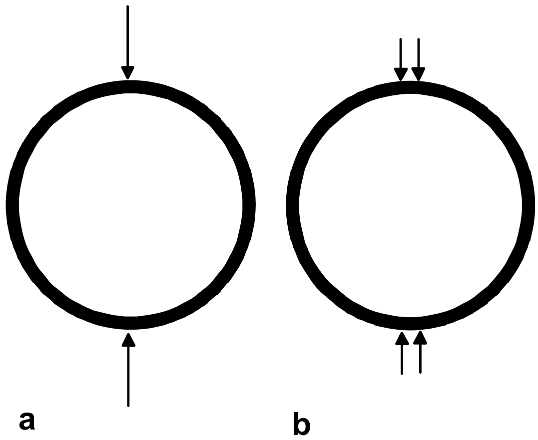

Fig. 8. Two-point loading and four-point loading on the liner. (a) Two-point loading and (b) Four-point loading.

5.3. Effect of angular expansion of the fracture on circumferential bending strains

While the mesh shown in Figs. 3 and 4 successfully captures both the deformed shape of the tight fitting host pipe–liner system and the local bending strains in the flexible liner, the locations of the local contacts deserve further discussion. When the pipe begins to deform, the local contacts are at exactly the crown and the invert of the liner, and there is a two-point or "parallel plate" loading condition, Fig. 8a. As the pipe deforms and the fracture opens, the local contacts separate to form four point loads on the liner, one pair each at the crown and invert, as illustrated on Fig. 8b.

In the previous analysis, joints with high normal stiffness and negligible shear stiffness were used to model the local contacts between the host pipe and the liner (Fig. 4). As θ increases, the joints connecting the liner and the host pipe rotate. However, the two joints modeling the local contacts are still connected to the liner exactly at the crown and invert, and forces are still transferred to the liner at those locations as two-point loading. Therefore, the effect of four-point loading on the liner is not correctly captured.

To study the effect of the pair of vertical forces that develops at crown and invert on the liner response, two additional finite element analyses were undertaken. The first analysis features a liner with the same dimensions and material properties as the previous analysis, subjected to two-point loading. A 7.2 mm displacement was prescribed at the crown, and the same amount was prescribed at the invert (Fig. 9a), resulting in final vertical deformation of

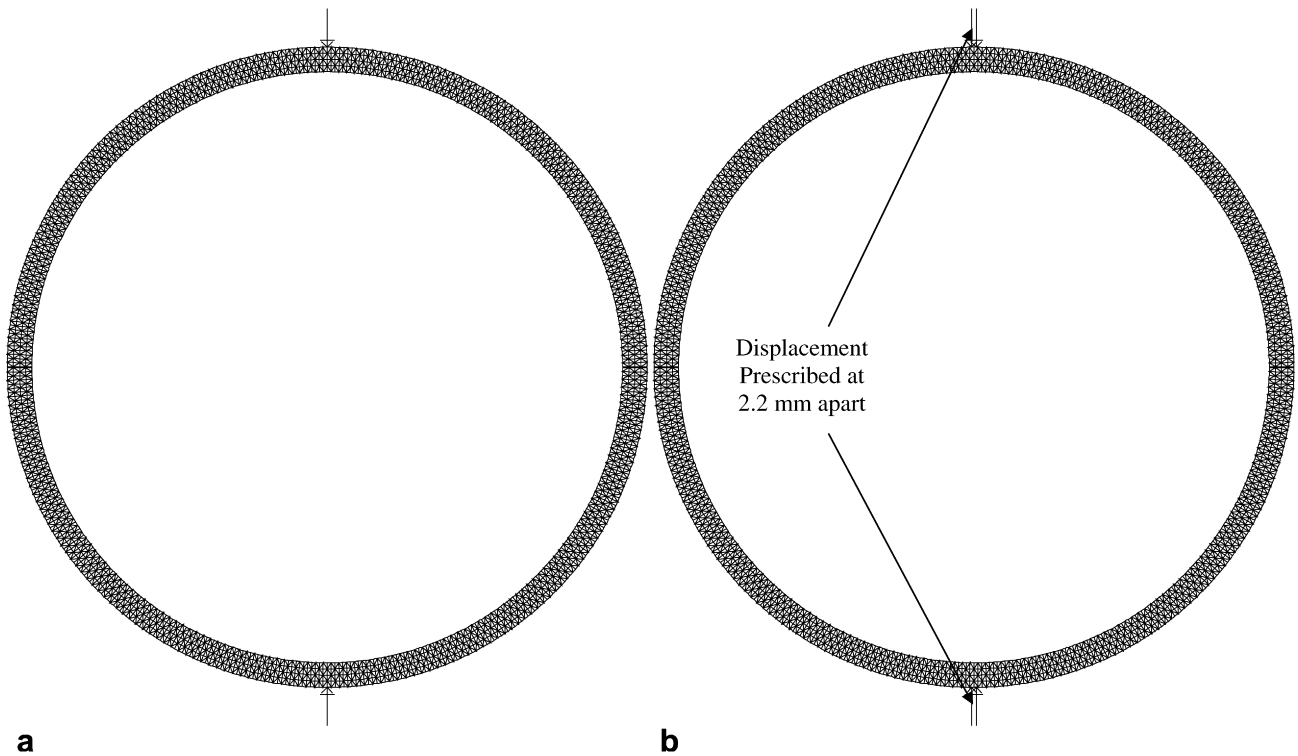

Fig. 9. Finite element meshes for the liner. (a) Single loads at crown and invert and (b) Double loads at crown and invert.

14.4 mm. Close to two thousand six-node triangular elements were used to model the whole liner.

The second analysis features the same liner, but subjected to four-point loading. At the crown, a pair of 7.2 mm displacements was prescribed 2.2 mm apart (Fig. 9b). This distance corresponds to the fracture angle of $\theta_{cr} = \theta_{inv} = 5°$; the same fracture angular expansion observed at $\Delta D_v =$ 14.4 mm (Table 3). The same displacement scheme is applied at the invert, resulting in final ΔD_v of 14.4 mm.

The analysis results reveal that when the liner is subjected to four-point loading, the local bending strains in the liner at the crown and invert are 3% less than those obtained from the two-point loading analysis. Not surprisingly, there was no significant effect on the bending strains at the springlines. It is concluded that for the deformation levels observed in the experiment, the angular expansion of the fracture and the development of a pair of contact forces at crown and invert has only a small effect on the local bending stains in the liner. The use of parallel plate loading effectively, and conservatively, represents the response of the liner encased in the host pipe.

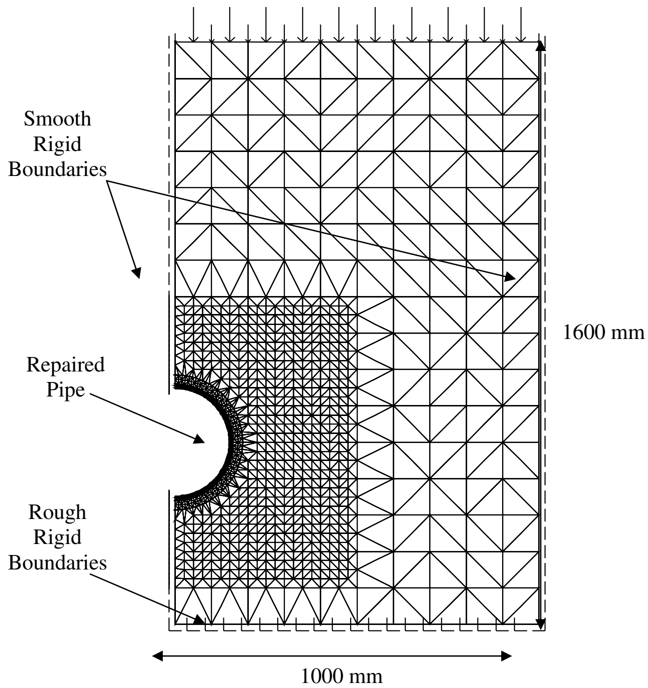

Fig. 10. Finite element mesh for test on buried host pipe–liner (Test 1).

6. Finite element analysis of buried pipe test

6.1. Modeling overview

To calculate the pipe deformations and the configuration of the laboratory tests, two-dimensional plane strain finite element analyses were undertaken. Two-dimensional plane strain conditions are a reasonable representation of the conditions in the pipe test because the test cell has very stiff, lubricated side-walls (Brachman, 1999). Only half of the biaxial test cell was analyzed due to symmetry. The side wall interface between the soil and the test cell was modeled as smooth and rigid, and a rough rigid boundary condition was modeled at the bottom of the test cell.

6.2. Analysis of test on repaired sewer pipe

For the fractured host pipe and the liner, the same mesh and material properties discussed earlier were used in this analysis (Fig. 3a). In addition, joint elements, 0.25 mm in length, were placed between the host pipe and the soil. Two cases have been investigated: a bonded pipe–soil interface condition and a full-slip pipe–soil interface condition. For the bonded condition, these joint elements were prescribed with both high normal and shear stiffnesses. Conversely, high normal stiffness and negligible shear stiffness were specified for analysis of the full-slip pipe–soil interface condition.

Close to nine hundred six-node triangles were used to model the backfill soil, and finer elements were used in the vicinity of the pipe (Fig. 10). The soil was modeled as an elastic–plastic solid, with a Mohr–Coulomb failure criterion and an associated flow rule (earlier studies indicate that dilation angle has little effect on buried pipe deformations, Moore and Booker, 1987). Cohesion of the soil was set to zero, and angle of internal friction, ϕ', of 41° was used (Lapos and Moore, 2002). To assess the performance of the analyses, comparisons are made to the laboratory measurements, where the finite element analyses use the values of secant soil moduli shown in Table 1 (calculated from laboratory measurements of settlement plate response and overburden pressure). The pipe deformations at each load step were calculated using the secant modulus at that particular load. The vertical pressure was applied at the top of the backfill soil using increments of 0.2 kPa.

The pipe deformations calculated for the bonded and full-slip host pipe–soil interfaces are shown in Fig. 11a and b, respectively. The vertical diameter change of the host pipe is not shown, since it is identical to the vertical diameter change of the liner as discussed previously.

Fig. 11a shows that when the host pipe and the soil is bonded perfectly, the calculated deformations at 165 kPa are about 60% less than the observed values in the laboratory. The reason for this large discrepancy is likely due to substantial errors at the springlines of the pipe. At that location, slip between the host pipe segments and the soil is likely to occur due to the fracture expansion at the outer surface. Forcing those joints to be bonded together yields substantial restraint, resulting in additional support against deformations. Analysis for full-slip produces calculated pipe deformations at 165 kPa that are within 10% of the measured values (Fig. 11b). The full-slip condition appears to be much closer to the interface condition operating in the test. While more sophisticated frictional interface modeling might be used to study the repaired pipe behaviour, it appears that good calculations result from the use of the 'smooth' or 'full-slip' idealization, and this is sufficient to explore the kinematics of lined sewer response under earth loads.

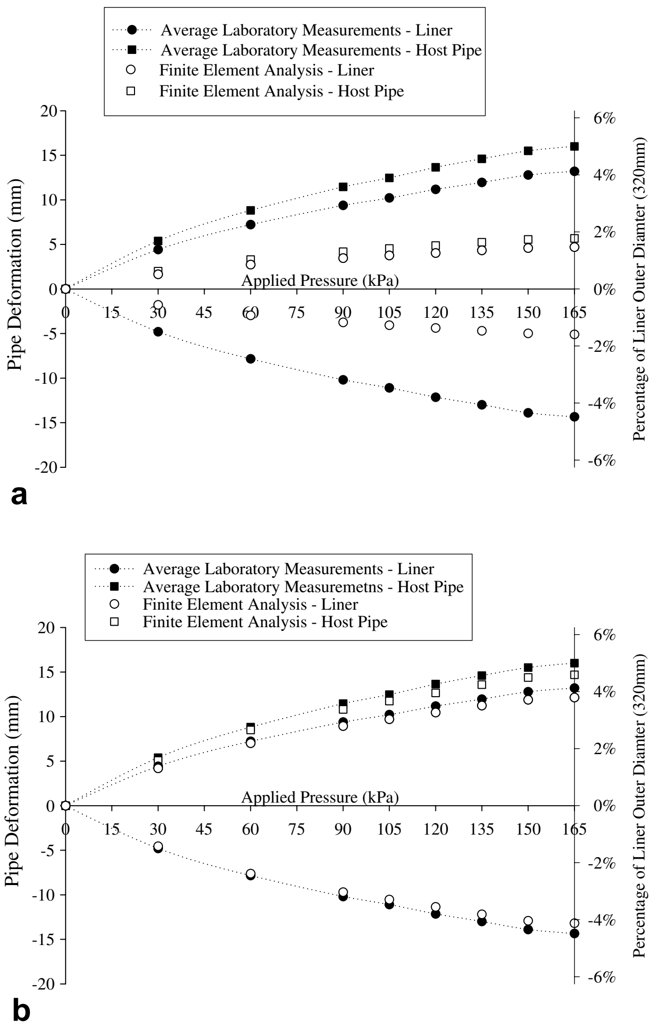

Fig. 11. Measured diameter changes versus finite element calculations. (a) Bonded host pipe–liner interface and (b) Host pipe–liner interface allowing full slip.

6.3. Effect of stress history on repaired pipe deformation

In the laboratory test, the host pipe was prefractured and lined ("repaired") before the application of earth loads. This loading scheme directly corresponds to a situation where surface live load or additional embankment material is placed on the ground surface across the top of a repaired sewer. However, one typical stress history associated with overburden pressure experienced by liners in the field features deterioration, fracturing, and deformation of the host pipe after it is lined (that is, earth loads acting on the outside of the repaired sewer pipe before it fractures). In particular, the liner may be installed within segments of host pipe that are not initially deformed or only partially deformed under earth loads. Subsequent deterioration of the soil envelope around the host pipe might then increase bending moments in the host pipe so it fractures, leading to diameter changes in the host pipe and local strains in the liner (Figs. 1a and 3a).

While this stress history was not explicitly reproduced in the laboratory test, it can be investigated using finite element analysis. The extent of local bending of the liner for host pipe deterioration and fracture after liner installation is therefore studied.

The mesh used was like that shown on Fig. 10. Two techniques were explored to temporarily restrain the host pipe against rotation at the fractures. First, a concrete "plug" ($E = 30$ GPa, $v = 0.3$), was numerically 'placed' inside the liner to minimize deformation during the application of the earth load. Identical to previous analyses, an overburden pressure of 165 kPa was applied at the surface of the backfill soil in 0.2 kPa increments. The "plug" was then removed after the full 165 kPa overburden pressure was applied.

The problem was also analyzed by temporarily placing high stiffness springs at the fractures to prevent the fractures from opening (at the inner boundary of the fractures at the crown and invert, and at the outer boundaries at the springlines). These additional springs were then removed when the full 165 kPa overburden pressure was applied, allowing the fractures to become active and the segmented pipe to deform.

Analysis results obtained with both these modeling approaches demonstrated that when the host pipe fractures are mobilized at 165 kPa, the amount of pipe deformations that then result are essentially identical to the prefractured host pipe–liner system under the same overburden pressure (the results are not included here since they could not be distinguished from the results for the prefractured host pipe analysis if added to Fig. 11).

When designing for the liner to sustain the local bending strains due to earth pressures, a decision is required regarding the amount of overburden pressure to consider. It is obvious that a liner is usually installed to restore the function of an already fractured host pipe, so that no liner strains will result unless there is subsequent disturbance. However, the liner may pass through certain sections of the host pipe where the fractures are only starting to develop, and where pipe deformations have not commenced or have only partly begun. Those sections then control liner design for the local bending limit state, since local bending can develop as the host pipe or surrounding soil deteriorate during the design life of the repair.

The finite element study has demonstrated that liner deformations develop in proportion to the full overburden pressure if the rigid sewer pipe fractures and deforms after liner installation. Safe liner designs should probably consider the full value of the geostatic earth pressures at the burial depth of the sewer unless steps are taken to prevent further deterioration of the host pipe and the surrounding soil over the design life of the repair.

7. Summary and conclusions

Recent work to study the static behavior of the tight fitting host pipe–liner system using numerical analysis has been presented. The analysis results given here are based on a specific set of repaired sewer configurations (geometries and materials). The kinematics of the host pipe–liner system have been examined using finite element analysis, where the fractures in the host pipe and local contacts between the host pipe and the liner were explicitly modeled.

Finite element analysis demonstrated that significant local bending can occur in the liner due to the local contacts between the host pipe and the liner. In addition, calculated circumferential stress and strain reveal that the liner is responding in almost pure bending when it is encased in a host pipe that can still carry hoop thrust. For the host pipe–liner configuration and the deformation level studied, examination of the deformed shape reveals that local contacts between the host pipe and the liner only occur at the crown and invert. Further analysis indicates that the angular expansion of the fractures and development of pairs of contact forces at the crown and invert has a negligible effect on the local bending in the liner. This means that ring theory considering the liner under parallel plate loading effectively captures the response.

Elasto-plastic finite element analyses of the buried pipe tests reveal that the host pipe–liner interface is closer to the full-slip interface condition than the bonded interface condition. The analysis results for the full-slip condition are within 10% of the measured values. It is likely that slip occurs at the springlines of the pipe where the facture open at the outer surface. If the host pipe and liner are artificially bonded together across the interface, the repaired pipe system is given additional stiffness to resist deformation that is unrealistic.

Elasto-plastic finite element analysis examining the influence of the stress history on the repaired sewer pipe has also been undertaken. The result indicates that a host pipe–liner system will deform under the full overburden pressure if the host pipe fractures after the liner is installed (as a result of degradation of the pipe material or the surrounding ground). Safe design of liners to resist the local bending strains will require consideration of liner deformations proportional to earth pressures associated with the full burial depth of the sewer, or actions to prevent further pipe or soil deterioration in sections where the liner passes through unfractured, undeformed segments of the host pipe.

Acknowledgement

This work was supported by the Natural Sciences and Engineering Research Council of Canada (NSERC), through the award of Postgraduate Scholarships to Dr. Law and a Discovery Grant to Dr. Moore. Test equipment was funded by NSERC and the Canada Foundation for Innovation. The work has benefited from the award of a Killam Research Fellowship to Dr. Moore through the Killam Bequest administered by the Canada Council of the Arts. His position at Queen's is funded through the Canada Research Chairs program.

References

ASTM, 1998. Standard practice for rehabilitation of existing pipelines and conduits by the inversion and curing of a resin-impregnated tube, F1216 – 93, ASTM, Philadelphia, PA.

Brachman, R.W.I., 1999. Mechanical Performance of landfill leachate collection pipes. Ph.D. Thesis, Faculty of Engineering Science, The University of Western Ontario, London, Canada.

Brachman, R.W.I., Moore, I.D., Rowe, R.K., 2001. The performance of a laboratory facility for evaluating the structural response of small diameter buried pipes. Canadian Geotechnical Journal 38, 260–275.

Carter, J.P., Balaam, N.P., 1980. AFENA – A General Finite Element Algorithm: User Manual, School of Civil and Mining Engineering, University of Sydney, N.S.W. 2006, Australia.

Dhar, A.S., Moore, I.D., 2000. Non-linear Analysis of buried HDPE pipe by the finite element method: comparison with laboratory test. In: Proceedings of GeoEng2000, Melbourne, Australia, November 19–24.

Digital Sewer Damage Catalogue due to the German Worksheet ATV-M 143-2 (08.01).

Doll, H., 2001. Dimensionierung von Kunststoff-linern – Close-fit-Verfahren'', Heft 59, Institut fü Grundbau, Bodenmechanik und Energiewasserbau, Universität Hannover.

Du, X., 1999. Interaction analysis of pipe–soil and liner–pipe–soil Systems. Master of Science Thesis, Louisiana Tech University, Ruston, Louisiana, USA.

El-Sawy, K., Moore, I.D., 1998. Stability of loosely fitted liners used to rehabilitate rigid pipes. Journal of Structural Engineering, ASCE 124 (11), 1350–1357.

European Standard, 2002. Guidance on the Classification and Design of Plastics Piping Systems Used for Renovation, EN 13689:2002, European Committee for Standardization.

Falter, B., Klein, J., 1989. Grenzlasten von Linern im Schachtbau. Bauingenieur 64, 9–18.

Falter, B., 2004. Lining stability: an analysis of damaged sewers. North American Society of Trenchless Technology, No Dig 2004, paper C-3-01, 11pp, New Orleans.

Lapos, B., Moore, I.D., 2002. Classification of strength and deformation parameters of Olimag synthetic olivine. In: Proceedings for the 55th Canadian Geotechnical Society annual Conference, Niagara Falls, Ont., Canada, October 20–23, 5pp.

Law, T.C.M., 2004. Behaviour of tight fitting flexible pipe liner under earth loads. Ph.D. Thesis, Faculty of Engineering Science, The University of Western Ontario, London, Canada.

Law, T.C.M, Moore, I.D., 2003. Behaviour and design of sewer liners for earth load. In: International No-Dig Conference, Las Vegas, Nevada, March 31–April 4, 15 pp.

Moore, I.D., Booker, J.R., 1987. Ground failure around buried tubes. International Journal of Rock Mechanics and Rock Engineering 20 (4), 243–260.

Moore, I.D., Hu, F., 1996. Linear viscoelastic modelling of profiled high density polyethylene pipe. Canadian Journal of Civil Engineering 23 (2), 395–407.

Takahashi, Y., Deguchi, T., Li, L., Hibara, T., Yamada, K., 2002. A study on the bedding effects of deteriorated existing sewage pipes on the close-fit non-bonded flexible linings and its mechanism. In: Proceedings of the International NO-DIG 2002 Conference, Copenhagen, Denmark, 13 pp.

Young, O.C., Trott, J.J., 1984. Buried Rigid Pipes: Structural Design of Pipelines. Elsevier Applied Science Publishers, 234 pp.